remote sensing

MDPI

Article

Hyperspectral Reflectance and Machine Learning Approaches for the Detection of Drought and Root–Knot Nematode Infestation in Cotton

Purushothaman Ramamoorthy [1], Sathishkumar Samiappan [1], Martin J. Wubben [2], John P. Brooks [2], Amrit Shrestha [3], Rajendra Mohan Panda [1], K. Raja Reddy [4] and Raju Bheemanahalli [4,*]

[1] Geosystems Research Institute, Mississippi State University, Mississippi State, MS 39762, USA
[2] USDA-ARS, Genetics and Sustainable Agriculture Research Unit, Mississippi State, MS 39762, USA
[3] Department of Agricultural and Biological Engineering, Mississippi State University, Mississippi State, MS 39762, USA
[4] Department of Plant and Soil Sciences, Mississippi State University, Mississippi State, MS 39762, USA
* Correspondence: rajubr@pss.msstate.edu

Abstract: Upland cotton encounters biotic and abiotic stresses during the growing season, which significantly affects the genetic potential of stress tolerance and productivity. The root-knot nematode (RKN) (*Meloidogyne incognita*) is a soilborne roundworm affecting cotton production. The occurrence of abiotic stress (drought stress, DS) can alter the plant–disease (RKN) interactions by enhancing host plant sensitivity. Experiments were conducted for two years under greenhouse conditions to investigate the effect of RKN and DS and their combination using nematode-resistant (Rk-Rn-1) and nematode susceptible (M8) cotton genotypes. These genotypes were subjected to four treatments: control (100% irrigation with no nematodes), RKN (100% irrigation with nematodes), DS (50% irrigation with no nematodes), and DS + RKN (50% irrigation with nematodes). We measured treatments-induced changes in cotton (i) leaf reflectance between 350 and 2500 nm; and (ii) physiology and biomass-related traits for diagnosing plant health under combined biotic and abiotic stresses. We used a maximum likelihood classification model of hyperspectral data with different dimensionality reduction techniques to learn RKN and DS stressors on two cotton genotypes. The results indicate (i) the RKN stress can be detected at an early stage of 10 days after infestation; (ii) RKN, DS, and DS + RKN can be detected with an accuracy of over 98% using bands from 350–1000 nm and 350–2500 nm. The genotypes 'Rk-Rn-1'and 'M8' showed differential responses to DS, RKN, and DS + RKN. With a few exceptions, all three stressors reduced the pigments, physiology, and biomass traits and the magnitude of reduction was higher in 'M8' than 'Rk-Rn-1'. Observed impact of stressors on plant growth followed DS + RKN > DS > RKN. Similarly, leaf reflectance properties exhibited a significant difference between individual stress treatments indicating that the hyperspectral sensor data can be used to discriminate RKN-infected plants from drought-stressed plants. Thus, our study reveals that hyperspectral and physiological changes in response to RKN and DS could help diagnose plant health before visual symptoms.

Keywords: drought stress; hyperspectral reflectance; *Meloidogyne incognita*; southern root–knot nematode

check for updates

Citation: Ramamoorthy, P.; Samiappan, S.; Wubben, M.J.; Brooks, J.P.; Shrestha, A.; Panda, R.M.; Reddy, K.R.; Bheemanahalli, R. Hyperspectral Reflectance and Machine Learning Approaches for the Detection of Drought and Root–Knot Nematode Infestation in Cotton. *Remote Sens.* **2022**, *14*, 4021. https://doi.org/10.3390/rs14164021

Academic Editors: Alessandro Matese and Giovanni Avola

Received: 14 July 2022
Accepted: 17 August 2022
Published: 18 August 2022

1. Introduction

Meloidogyne incognita (southern root-knot nematode, RKN) is one of the most important plant-parasitic nematodes affecting cotton production in the United States [1]. The estimated cotton yield in the United States during 2015 was about 7.9 million bales, but losses due to RKN were estimated at approximately 215,500 bales with an estimated value of $73.94 million [2,3]. RKN has many hosts including weeds and field crops [4,5], where it feeds on and lives in plant roots or inhabits the rhizosphere. RKN second-stage juveniles

(J2) preferentially infect the root tips and migrate intercellularly through the root vasculature. The J2 then becomes sedentary near the endodermis where it elicits the formation of multiple 'giant cells' that provide the developing nematode with nutrients throughout the life cycle. Vascular tissue surrounding the giant cells undergo extreme hypertrophy and forms the characteristic 'galls' seen on RKN-infected roots [6]. Giant cell formation of galls is solely to benefit the nematode, not the host, and provide the necessary nutrition for the growth and subsequent production of large numbers of eggs. RKN-induced feeding sites are nutritional sinks that impede the total supply of water and nutrients to the shoot, reducing crop growth and yield in cotton [7,8], and other crops [9]. Various management practices like nematicide application, fumigation and soil solarization are implemented to control RKN infection [10]. However, considering the cost, soil health, and safety, these management practices are not adapted to large-scale farming. Methods like crop rotation, biological control, and resistant varieties are considered economical, sustainable, and eco-friendly options to control the RKN effect on crops [10,11]. Though substantial progress has been made in developing host–plant resistance, significant gaps exist due to the complexity of plant–nematode interaction mechanisms [12,13].

Field-grown crops have the possibility of experiencing multiple stresses simultaneously, such as a combination of abiotic and biotic stresses [14]. This combination is common to agricultural areas worldwide that impact crop productivity. More than 65% of cotton in the United States was grown under rainfed conditions [15]. With the increasing threat of climate change, access to irrigation is decreasing, further turning the irrigated cultivated land into rainfed [16]. Many of the rainfed cotton-growing fields are abundant with the increased RKN populations. Plants produce reactive oxygen species as signaling molecules to control pathogen infection [17]; however, inadequate soil moisture weakens this defense mechanism [18,19]. A stressor (like drought) enhances RKN spread, making the plant more susceptible to pathogen infection leading to significant yield reduction. In particular, RKN infection causes substantial damage to roots by disrupting xylem, phloem, epidermis, and cortical tissues [20,21]. RKN infection symptoms are similar to those often attributed to drought stress, where plants exhibit premature wilting, nutrient deficiency, and stunted growth [10,22]. These abnormalities appear in the infected plants due to reduced water uptake and poor water supply to the shoots. This event results in decreased stomatal conductance and net photosynthesis, thereby increasing canopy temperature, which is comparable to plants' experiencing drought stress [23–25]. Exposure of plants to RKN can alter plant metabolism and contribute to premature leaf abscission, which is presumed to affect chlorophyll content and photosynthesis in soybean [26]. Growth is substantially reduced by infection with RKN [23], similar to drought in cotton [24,27].

Early diagnosis of stressors is required to reduce disease spread and facilitate real-time management practice. Recent studies demonstrated that crops share common physiological changes in response to RKN and drought stress [10,22]. However, changes in leaf spectral properties specific to RKN or drought stress are not yet investigated in many crops, including cotton. Recent advancements in remote sensing (multispectral and hyperspectral) can help early diagnosis of stressors before the plant's visual symptoms appear. Hyperspectral data contain reflectance as hundreds of narrow spectral bands in visible and infrared regions. Hyperspectral sensors have proven to help distinguish subtly different levels of plant stress. In the literature, the hyperspectral data are shown to have the ability to rapidly and early detect various biotic- and abiotic-stress symptoms [28,29]. Stressors alter the optical properties of leaves by changing the leaf pigments, cell structure, water content, leaf physiology, and chemical composition. In response to stressors, plants adjust their leaf optical properties to balance light reflectance, absorption, and transmittance [30,31]. Ground-based sensing of leaf reflectance data measured using spectroradiometers and hyperspectral sensors have a higher potential of discriminating even small differences between the stressed and non-stressed plants due to its richness in a larger number of discrete wavelengths [32,33]. However, hyperspectral data contain highly correlated narrow spectral bands that demand a larger number of training samples to accurately determine class conditional probabilities that are required in statistical machine learning (ML) modeling. The application of dimensionality reduction algorithms can alleviate the small training size issues. ML-based techniques in agriculture have shown the potential to discriminate healthy plants from the stressed ones caused by either RKN [32] or drought stress [34] using the hyperspectral signatures. Several studies have shown that changes in physiology and biochemical processes in response to a broad range of stressors, such as drought, temperature, salinity, nutrient and diseases, can be identified using leaf reflectance properties [35–39]. However, identifying unique and shared spectral profile changes for a broad range of stressors require multidisciplinary approaches.

Hyperspectral imagery records reflectance values over a wide range of continuous narrow spectral bands in the visible and infrared regions. This results in high-dimensional data providing helpful information for land-cover classification, target recognition, and mapping [40,41]. This high dimensionality in hyperspectral imagery often suffers from a Hughes phenomenon [42] that results in poor performances in statistical pattern classification tasks with small sample size. A suitable dimensionality reduction procedure regulates these problems of high dimensionality in hyperspectral image analysis. This method of dimensionality reduction deals with data compression and feature extraction for classification [43]. This reduction process is based on projections and decision rules optimizing a global criterion such as the overall accuracy (OA) or Fisher's ratio [44]. Principal component analysis (PCA) and Fisher's linear discriminant analysis (FLDA) are popular methods for such dimensionality reduction and have been widely applied in hyperspectral imagery analysis [40,41,43,45]. In general, FLDA has greater efficiency in feature reduction and classification than PCA and is preferred in hyperspectral data analysis [46]. Stepwise linear discriminant analysis (SLDA) mitigates the effects of a small sample size on its transformations, where forward selection and backward rejection determine the best feature subset. In this study, we are not only interested in identifying the changes in leaf spectral properties in response to individual and combined drought and RKN stresses. We also sought to determine the suitability of a spectral signatures-based screening approach to distinguish stressed plants from healthy ones and to forecast the type of stress the plants undergo (drought or RKN) before the visual symptoms appear.

Therefore, the present study aims to (i) assess the individual and interactive effects of RKN and drought on the physiology and growth of two cotton genotypes; (ii) compare the ability of statistical ML methods in discriminating or classification of healthy plants from stresses under individual and interactive RKN and drought stress treatments; and (iii) determine the best ML classifier and dimensionality reduction approach for early diagnosis of stressors in cotton grown in a greenhouse controlled experiment.

2. Materials and Methods

2.1. Crop Husbandry

Two cotton genotypes, 'Rk-Rn-1' (nematode resistant; [47]) and 'M8' (nematode susceptible), were used in this study. The experiments were carried out during the years 2020 (year 1) and 2021 (year 2) in a controlled environment greenhouse facility at the USDA—ARS, Mississippi State, MS, USA. Two seeds were sown at a depth of about 2–3 cm in a pot containing a mixture of field soil and sand (1:1 ratio). The seedling was thinned to one per pot at the two-leaf stage. Five replications were maintained for each genotype per treatment ($5 \times 2 \times 2 = 20$ pots) in year 1, and ten replications were maintained for each genotype per treatment ($10 \times 2 \times 4 = 80$ pots) in year 2. The temperature in the glasshouse was maintained at 30/20 °C (day/night) and 60–70% relative humidity with a photoperiod of 11/13 h (day/night) during the experiment. The soil moisture was monitored using a handheld moisture meter (Theta Probe ML2x, Delta-T Devices, Cambridge, UK).

2.2. Treatment

A *M. incognita* race 3 population was cultivated on susceptible cotton plants. RKN eggs used for inoculum were collected from infected cotton roots [48]. In year 1, the experiment contains two treatments (control and nematode stress). (1) control—100% irrigation [0.15 m^3 m^{-3} volumetric water content (VMC)] and no nematode inoculation; (2) nematode stress—100% irrigation. Pots receiving RKN inoculum were inoculated with 50,000 RKN eggs ten days after planting. RKN eggs were applied as 10 × 1 mL aliquots into 10 holes surrounding the plant.

In year 2, the experiment contained four treatments: (1) control—100% irrigation, no nematode inoculation; (2) drought stress (DS)—40% irrigation (0.060 m^3 m^{-3} VWC), no nematode inoculation; (3) root-knot nematode stress (RKN)—100% irrigation and nematode inoculation (100,000 RKN eggs); (4) drought and nematode stress (DS + RKN)—40% irrigation and nematode inoculation. As with the year 1 experiment, pots receiving RKN inoculum were inoculated ten days after planting. Approximately 100,000 RKN eggs were applied as 10 × 1 mL aliquots into 10 holes surrounding the plant. The approximate number of RKN eggs per cm^3 of soil was equivalent between years 1 and 2. Successful RKN infection of the susceptible control plants was confirmed at the end of the experiments by the appearance of extensive RKN-induced root galling.

2.3. Data Collection

2.3.1. Physiological and Shoot Biomass Traits

Chlorophyll content and nitrogen balance index were measured on a fully opened mainstem leaf, third leaf from the terminal, across all treatments using a handheld Dualex® scientific instrument (Force A DX16641, Paris, France) at 80 days after planting (DAP) or 60 days after stress in year 1 and multiple times (16, 24, 32, 39, 46, 53, and 72 days after stress) in year 2. A portable handheld LI-600 porometer system integrated with a fluorometer (LI-COR Biosciences, Lincoln, NE, USA) was used to measure stomatal conductance and transpiration across all treatments between 10:00 a.m. and 12:00 p.m. in year 1 (60 days after stress) and year 2 (16, 24, 32, 39, 46, 53, and 72 days after stress). Plants were harvested at 60 days after stress in year 1 and 72 days after stress in year 2. Plants were kept in a forced-air oven at 75 °C for three days to determine root and shoot dry weights.

2.3.2. Leaf Hyperspectral Reflectance

Leaf hyperspectral reflectance (350 and 2500 nm) data were collected between 10:00 a.m. and 12:00 p.m. in year 1 (10, 30 and 60 days after stress) and year 2 (32, 39, 46, 53, and 72 days after stress), using a PSR + 3500 spectroradiometer (Spectral Evolution, Haverhill, MA, USA). The spectroradiometer is attached to a leaf clip probe with an internal calibrated light source. The instrument's spectral range is 350–2500 nm (2150 bands) with a spectral resolution of 2.8 nm at 700 nm, 8 nm at 1500 nm, and 6 nm at 2100 full width at half maximum resampled to produce data at 1 nm. Five instantaneous spectral reflectance measurements were recorded from the adaxial surface in each treatment for each genotype and treatment by keeping the leaf vertical to the optical probe. Each measurement is an average of 10 readings in years 1 and 2. At the beginning of each treatment, a white reference measurement was taken, and each measurement was then radiometrically calibrated based on the white reference.

2.4. Statistical Machine Learning

A maximum likelihood (ML) classifier with a dimensionality reducer approach was used to classify leaf hyperspectral signatures. This setup has shown to effectively classify subtly different classes in hyperspectral data in reduced dimensions without suffering from the Hughes phenomenon. The maximum likelihood classifier assumes that the statistics for each class in each hyperspectral band usually are distributed and computes the probability that a given pixel belongs to a particular class [45]. The different dimensionality reduction algorithms used in this study to differentiate RKN stressed cotton leaf reflectance from drought and control treatments were PCA, FLDA, and SLDA [32]. FLDA and PCA are closely related because they are both linear; however, the method of learning in PCA is unsupervised, while it is supervised in FLDA. The PCA finds the direction of the largest variations without paying attention to the class structure. PCA minimizes the mean square error between observed and predicted vectors. On the other hand, FLDA maximizes the ratio between or within classes and discriminates against the class structure by maximizing the distance and minimizing the variation between classes. PCA and FLDA are intuitive to understand and have shown to be effective in preserving discrimination features in subtly different classes. The samples within each class have the smallest possible scatter at maximum ratio and the most distance between the classes.

The classification analysis was done for the entire set of bands (350–2150 nm) and a range of bands (350–1000 nm) to understand the utilities of the small number of bands to classify RKN and drought stressors. The choice of 350–1000 nm stemmed from the fact that cost-effective, commercially available drone mountable hyperspectral sensors cover this region. Temporal misalignment experiments were conducted to determine if the information contained in hyperspectral data is sufficient to train a ML model with one date and test it later. This analysis will be helpful in deciding on the changes in leaf spectrum between days after stresses and reduce the efforts of ground truth acquisition. Classification accuracy for every four traits was derived, and the OA was compared with the Kappa statistics [49].

3. Results and Discussion

3.1. Physiological Traits

Reduced water transportation from the root to the shoot may cause DS in plants and limit nutrient flow [50]. Unlike DS, there is little information on the effects of nematode parasitism on cotton physiology [7]. The cultivar and treatment were significantly varied ($p < 0.05$) for both pigment and physiological traits except for chlorophyll and NBI in year 2. The chlorophyll content is a valuable screening proxy to detect stress effects and plant health [51]. In this study, the magnitude of reduction for chlorophyll and NBI were higher in 'M8' compared to 'Rk-Rn-1' in year 1 (Figure 1A,C). RKN stresses 'M8' plants showed significant ($p < 0.05$) reduction in chlorophyll and NBI compared to control in year 1. Nematodes that live in RKN-infected plant roots consume a portion of the nutrients that are supplied to the plants. As reported in other studies, this could cause nutrient stress in plants, ultimately results in low leaf nitrogen [25,52]. The nematode entry into 'Rk-Rn-1' roots had minimal effect on transpiration and stomatal conductance compared to the DS, as the reduction in transpiration and stomatal conductance due to DS and DS + RKN stresses were statistically significant ($p < 0.05$). A similar observation was also observed in the previous research [7]. Maintaining optimum transpiration under stress is a good indication of normal stem water flux. The reduced transpiration on nematode-infected plants during high evaporative demand suggests a higher hydraulic resistance than the control plants [23]. In this study, the genotype 'Rk-Rn-1' maintained relatively high transpiration and stomatal conductance compared to genotype 'M8', indicating that the RKN-resistant genotype has less hydraulic resistance than the RKN-susceptible genotype.

The DS had a substantial negative effect on leaf functional parameters in both genotypes; however, the stressors had a higher impact on the 'M8' genotypes than the 'Rk-Rn-1'. Regardless of DS or RKN, traits closely related to plant–water transport (transpiration and stomatal conductance), rather than other traits (pigments), are clearly depicting the negative influence on plant health. These findings demonstrated that DS induced changes in water loss could further amplify [53] the impact of RKN infection regardless of the plant's sensitivity to nematode stress. Several studies reported that DS decreases leaf chlorophyll content in various crops [54,55]. We found a similar reduction in 'Rk-Rn-1' chlorophyll content in response to DS; however, no such decremental pattern was observed when the drought coincided with RKN stress. Based on this observation, we anticipate that RKN stress-induced galls act as a nutrient sink that redirects some nutrients in the RKN-resistant cotton cultivar [22], concealing the detrimental effect caused by DS on chlorophyll content.

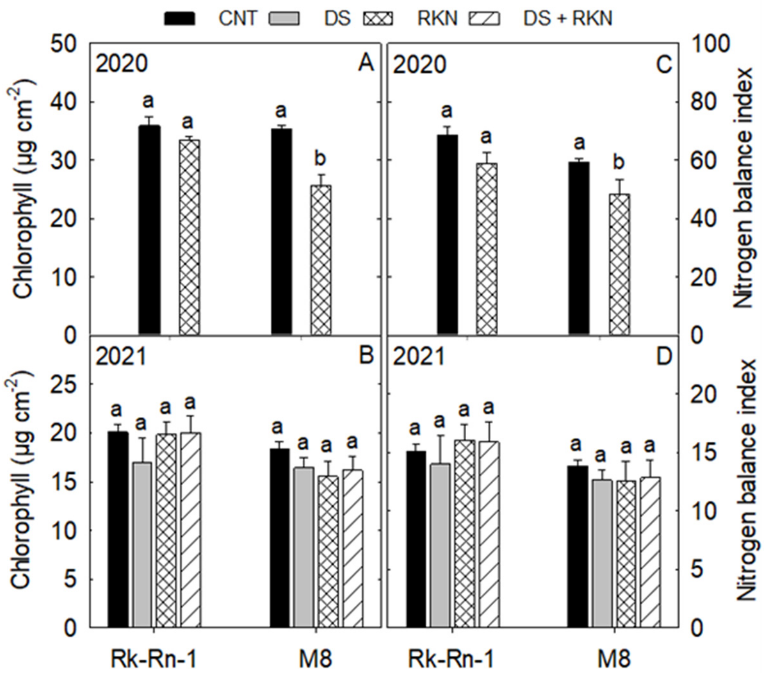

Figure 1. Drought and nematode effects on chlorophyll content (**A**,**B**) and nitrogen balance index (**C**,**D**) of cotton genotypes (Rk-Rn-1 and M8) measured under control (CNT), drought stress (DS), nematode stress (RKN), and DS + RKN combination in 2020 (**A**,**C**) and 2021 (**B**,**D**). Vertical bars denote mean ± SE. Means followed by a common letter are not significantly different by Duncan's multiple range test at the 5% level of significance.

Both genotypes and treatments showed markable variation for the chlorophyll content, NBI, transpiration and stomatal conductance measured at various growth stages (16, 24, 32, 46, 53, and 72 days after inoculation) in year 2 (Figures S1 and 2). Despite differences in pigments and physiology between genotypes and treatments, we can see a clear decreasing pattern in chlorophyll and NBI from 16 to 72 days after stress (Figure S1A,B). The reduction in chlorophyll content was about 45% in 72 days after stress compared to 16 days after stress treatment, when averaged across genotypes and treatments (Figure S2A,B). Our results imply that physiology parameters, rather than pigments, have the ability to distinguish DS and DS + RKN stressed plants from control plants. There was precise separation observed under RKN stress since the reduction depends on the cultivars' sensitivity. Overall, the genotype 'Rk-Rn-1' maintained a better physiological status compared to 'M8'.

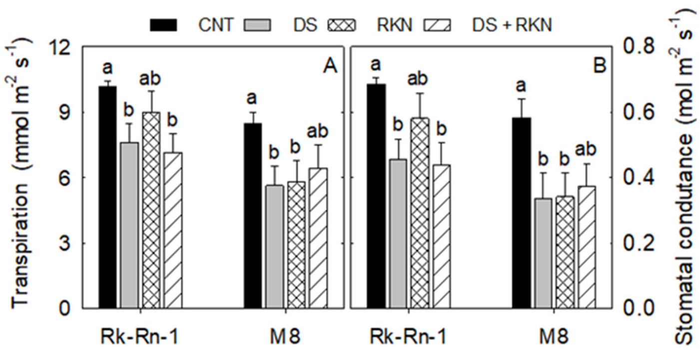

Figure 2. Drought and nematode treatments effects on (**A**) transpiration (mmol m^{-2} s^{-1}); (**B**) stomatal conductance (mmol m^{-2} s^{-1}) of cotton genotypes (Rk-Rn-1 and M8) measured under control (CNT), drought stress (DS), nematode stress (RKN), and DS + RKN combination in 2021. Vertical bars denote mean ± SE. Means followed by a common letter are not significantly different by Duncan's multiple range test at the 5% level of significance.

3.2. Biomass

Both physiological and biochemical parameters influence leaf photosynthesis, which ultimately determines the biomass accumulation in plants [56,57]. Any disruption in these parameters by single or multiple stresses can cause a significant reduction in biomass production [14,58]. Under control condition, the genetic potential of both genotypes was similar for shoot dry weight (Figure 3). The shoot dry weight was significantly reduced in response to both individual and combined stresses ($p < 0.05$) compared to their control counterparts (Figure 3) except under RKN stress in year 2 (Figure 3B).

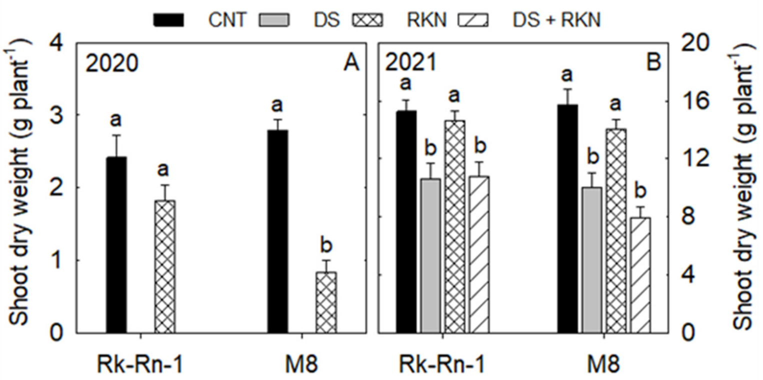

Figure 3. Drought and nematode effects on shoot dry weight (**A**,**B**) of cotton genotypes (Rk-Rn-1 and M8) measured under control (CNT), drought stress (DS), nematode stress (RKN), and DS + RKN combination in 2020 (**A**) and 2021 (**B**). Vertical bars denote mean ± SE. Means followed by a common letter are not significantly different by Duncan's multiple range test at the 5% level of significance.

The genetic potential of 'M8' for root growth was about one-fold greater than that of the genotype 'Rk-Rn-1' under control (Figure S3), but when 'M8' was exposed to RKN stress, its total root length was significantly reduced ($p < 0.05$). For example, the nematode stressed genotype 'Rk-Rn-1' increased its total root length by 4% and 20% of its root dry weight compared to the control. RKN-infected plants seem to be momentarily investing more in their root growth in response to RKN treatment [59]. It is conceivable that the increased root length and root dry weight in 'Rk-Rn-1' is a form of insurance, compensating for a temporary loss of functionality in infected roots [60]. In response to RKN, the genotype 'M8' decreased its total root length (50%) and root dry weight (36%). Unlike root length, root dry weight did not differ between genotypes under RKN stress. This could be due to higher sensitivity of 'M8' to RKN stress that possibly increased the number of galls formed, thereby increasing its root dry weight [61] as equal to that of 'Rk-Rn-1'.

Though both genotypes produced less shoot dry weight in response to RKN stress, the magnitude of reduction in shoot dry weight was three-fold higher in 'M8' (70%) than 'Rk-Rn-1' (24%) in year 1, whereas the reduction in response to RKN in year 2 was mini-mal for 'Rk-Rn-1' (4%) and 'M8' (11%). DS and DS + RKN had a substantial negative effect on shoot biomass in both 'Rk-Rn-1' (31% and 29%) and 'M8' (36% and 50%) (Figure 3B). Studies suggested that RKN stress in cotton reduces water flow in the plant, causing temporary wilting similar to DS [10,22]. The current study results generally suggest that the quantitative differences in the variables affected (shoot and root traits) and the magnitude of effects caused by the stressors are not identical.

3.3. Variation in Spectral Reflectance in Response to Stressors

Overall accuracy in the 0–100% range is often used to assess classifier performance, class accuracies, and Kappa statistics. A Kappa value ≤ 0 indicates no agreement, 0.01–0.20 as none to slight, 0.21–0.40 as fair, 0.41–0.60 as moderate, 0.61–0.80 as substantial, and 0.81–1.00 as almost perfect agreement [62].

The leaf reflectance signatures measured at 10, 30, and 60 days after stress in year 1 were classified using ML with two classes (RKN stress and control) with PCA, FLDA, and SLDA, which had a best overall OA of 95% (Kappa = 0.89) (Table 1). Similarly, the leaf reflectance signatures measured at 16, 24, 32, 46, 53, and 72 days after stress in year 2 were classified using ML with four and eight classes with the three-dimensionality reducers, with the best OA of 99% (Kappa = 0.96) and 98% (Kappa = 0.97), respectively (Tables 2 and 3). The Kappa values ranged from 0.84 to 0.96 in year 1 and from 0.91 to 0.98 in year 2, indicating the robustness and reliability of treatment classification.

Table 1. Classification accuracies for a two-class problem (M8 vs. Rk-Rn-1) using leaf spectral reflectance information between 350–1000 nm and 350–2500 nm measured at 10, 30, and 60 days after stress treatment in 2020.

Days after Stress	Class Accuracy	M8						Rk-Rn-1					
		PCA		SLDA		FLDA		PCA		SLDA		FLDA	
		350–1000 nm	350–2500 nm	350–1000 nm	350–2500 nm	350–1000 nm	350–2500 nm	350–1000 nm	350–2500 nm	350–1000 nm	350–2500 nm	350–1000 nm	350–2500 nm
10	Control	96	96	100	92	80	68	100	100	100	88	72	52
	RKN	96	92	96	100	68	32	96	100	96	92	52	68
	OA	96	94	98	96	74	50	98	100	98	90	62	60
	Kappa	0.92	0.88	0.96	0.92	0.48	0.0	0.96	1.0	0.96	0.80	0.24	0.20
30	Control	95	100	95	95	95	57	96	100	98	92	72	4
	RKN	96	96	100	100	64	72	100	96	100	88	80	76
	OA	96	98	98	94	78	65	98	98	98	90	76	40
	Kappa	0.91	0.96	0.96	0.87	0.57	0.29	0.96	0.96	0.96	0.92	0.52	−0.20
60	Control	87	87	93	93	53	40	100	96	96	100	84	80
	RKN	100	100	100	100	84	84	96	96	96	96	88	80
	OA	95	95	98	98	73	68	98	96	96	98	86	80
	Kappa	0.89	0.89	0.89	0.95	0.39	0.26	0.96	0.92	0.92	0.96	0.72	0.80

PCA = Principal component analysis; SLDA = Stepwise linear discriminant analysis; FLDA = Fisher's linear discriminant analysis; OA = Overall accuracy.

Table 2. Classification accuracies for a four-class problem (control, drought stress (DS), root–knot nematode (RKN) stress, and DS + RKN stress combination) using leaf spectral reflectance information between 350–1000 nm and 350–2500 nm measured of two cotton genotypes (M8 and Rk-Rn-1) at 32, 39, 46, 53, and 72 days after stress treatment in 2021.

Days after Stress	Class Accuracy	M8						Rk-Rn-1					
		PCA		SLDA		FLDA		PCA		SLDA		FLDA	
		350–1000 nm	350–2500 nm	350–1000 nm	350–2500 nm	350–1000 nm	350–2500 nm	350–1000 nm	350–2500 nm	350–1000 nm	350–2500 nm	350–1000 nm	350–2500 nm
32	Control	96	96	96	98	96	98	96	98	94	100	100	100
	RKN	100	100	95	98	100	91	100	100	98	96	89	98
	DS	100	94	83	85	100	96	94	98	92	96	98	94
	DS + RKN	98	100	98	100	98	93	98	100	98	100	85	89
	OA	99	96	93	90	99	97	96	98	95	95	92	92
	Kappa	1.0	0.97	0.90	0.93	1.0	0.92	0.98	0.99	0.94	0.97	0.90	0.93
39	Control	98	98	100	96	100	100	98	94	100	96	100	100
	RKN	98	98	100	100	94	94	100	100	100	100	91	92
	DS	100	100	94	89	98	98	98	98	94	96	96	92
	DS + RKN	98	98	98	98	94	93	98	98	100	100	98	98
	OA	99	98	98	95	97	95	99	97	98	97	96	94
	Kappa	1.0	0.98	0.97	0.94	1.00	0.97	0.98	0.97	0.98	0.97	0.95	0.94

Table 2. *Cont.*

Days after Stress	Class Accuracy	M8						Rk-Rn-1					
		PCA		SLDA		FLDA		PCA		SLDA		FLDA	
	Control	98	98	96	100	100	100	98	98	96	98	100	100
46	RKN	100	98	80	83	94	96	98	98	100	100	88	94
	DS	99	100	100	100	94	95	98	98	91	86	98	98
	DS + RKN	99	99	98	96	98	99	100	100	98	100	94	94
	OA	99	98	94	96	96	93	99	98	96	94	95	95
	Kappa	1.0	0.98	0.92	0.93	0.90	0.96	0.98	0.98	0.95	0.94	0.93	0.95
	Control	98	96	96	94	100	100	98	98	98	94	100	100
53	RKN	98	98	100	100	92	89	100	98	100	100	89	89
	DS	98	98	82	94	98	96	98	97	94	94	96	94
	DS + RKN	100	100	98	100	96	98	100	98	98	98	94	96
	OA	99	97	93	97	97	93	99	98	98	95	95	94
	Kappa	1.0	0.97	0.91	0.96	1.0	0.94	0.99	0.97	0.97	0.95	0.93	0.93
	Control	98	98	94	94	93	96	98	98	96	98	98	100
72	RKN	100	98	97	88	91	94	100	98	97	100	93	94
	DS	88	98	80	94	93	96	88	98	78	86	89	96
	DS + RKN	100	100	100	98	92	96	100	100	97	100	93	100
	OA	96	97	92	93	92	88	96	99	91	96	93	98
	Kappa	0.95	0.98	0.89	0.91	0.90	0.94	0.95	0.98	0.87	0.94	0.91	0.97

PCA = Principal component analysis; SLDA = Stepwise linear discriminant analysis; FLDA = Fisher's linear discriminant analysis; OA = Overall accuracy.

Table 3. Classification accuracies on an eight-class problem (control vs. drought stress vs. RKN stress vs. genotypes) using leaf spectral reflectance information between 350–1000 nm and 350–2500 nm of two cotton genotypes (M8 and Rk-Rn-1) measured at 32, 39, 46, 53, and 72 days after stress treatment in 2021.

	Days after Stress/ Class Accuracy	PCA					SLDA					FLDA				
		32	39	46	53	72	32	39	46	53	72	32	39	46	53	72
Wavelengths (350–1000 nm)	M8–DS + RKN	92.6	98.0	98.0	95.2	97.8	94.3	100	96.2	96.2	97.8	100	100	100	100	100
	M8–RKN	97.9	98.0	98.0	98.0	100	100	98.0	100	100	100	87.7	92.5	92.5	92.5	88.0
	Rk-Rn-1–DS + RKN	98.0	100	98.0	100	90.0	92.5	96.1	98.0	94.3	79.0	100	98.0	98.0	98.0	100
	Rk-Rn-1–RKN	98.0	98.0	100	98.0	100	98.0	96.1	96.0	98.0	97.4	100	100	100	98.0	97.8
	M8–DS	100	96.0	98.0	100	95.7	98.0	96.1	95.7	96.0	99.8	94.2	94.3	90.9	94.3	95.7
	M8–control	97.8	98.0	100.0	94.2	95.7	100	100	94.1	96.0	97.8	95.4	97.9	100.0	97.9	89.8
	Rk-Rn-1–DS	98.0	98.0	98.0	98.0	97.7	98.0	100	96.1	98.0	97.7	98.0	98.0	98.0	98.0	95.5
	Rk-Rn-1–control	98.0	98.0	98.0	98.0	97.8	98.0	100	98.0	100	97.8	96.2	98.0	98.0	98.0	100
	OA	98.0	98.0	98.5	97.8	96.7	97.2	98.3	96.8	97.3	95.0	96.2	97.3	97.0	97.0	95.6
	Kappa	0.97	0.98	0.98	0.97	0.96	0.97	0.98	0.96	0.97	0.94	0.96	0.97	0.97	0.97	0.95
Wavelengths (350–2500 nm)	M8–DS + RKN	92.6	100	96.2	96.2	97.8	95.2	100	96.2	96.2	97.8	100	100	100	100	100
	M8–RKN	97.8	100	97.9	98.0	100	100	98.0	100	100	100	87.7	94.2	92.5	92.5	88.2
	Rk-Rn-1–DS + RKN	98.0	100	96.1	100	88.2	89.3	96.0	98.0	94.3	83.3	100	98.0	98.0	98.0	100
	Rk-Rn-1–RKN	96.2	98.0	98.0	96.2	97.7	98.0	96.0	96.0	98.0	97.5	100	100	100	98.0	97.8
	M8–DS	100	94.3	100	100	100	98.0	96.0	95.7	100	97.8	94.2	94.3	90.9	94.3	97.8
	M8–control	93.8	100	100	98.0	95.7	97.7	100	94.1	100	100	95.4	97.9	100	95.9	93.6
	Rk-Rn-1–DS	100	98.0	96.1	98.0	97.8	98.0	98.0	96.1	98.0	97.8	98.0	98.0	98.0	98.0	93.3
	Rk-Rn-1–control	98.0	98.0	98.0	98.0	100	98.0	100	98.0	100	97.8	96.2	100	98.0	98.0	100
	OA	97.0	98.0	97.8	98.0	96.9	96.7	98.0	96.8	98.3	96.1	96.2	97.8	97.0	96.8	96.1
	Kappa	0.97	0.98	0.97	0.98	0.97	0.96	0.98	0.96	0.98	0.96	0.96	0.97	0.97	0.96	0.96

RKN = Root–knot nematode; PCA = Principal component analysis; SLDA = Stepwise linear discriminant analysis; FLDA = Fisher's linear discriminant analysis; OA = Overall accuracy.

The above-mentioned experiments were conducted with two sets of hyperspectral bands, (1) 350–1000 nm; (2) 350–2500 nm; the OA and Kappa in both sets of experiments

(Table 4) were found to be excellent. The differences between classification accuracies are more minor compared to complementary treatments with all the spectral bands in year 1. The ability of ML to classify bands in 350–1000 nm demonstrates that RKN infection and DS symptoms may be mapped at the field level with a commercially available drone mountable hyperspectral sensor.

Table 4. Temporal misalignments in a two-class problem (M8 vs. Rk-Rn-1) using leaf spectral reflectance information between 350–1000 nm and 350–2500 nm of cotton genotypes measured at 10, 30, and 60 days after stress treatment in 2020.

Days after Stress	Class Accuracy	M8						Rk-Rn-1					
		PCA		SLDA		FLDA		PCA		SLDA		FLDA	
		350–1000 nm	350–2500 nm	350–1000 nm	350–2500 nm	350–1000 nm	350–2500 nm	350–1000 nm	350–2500 nm	350–1000 nm	350–2500 nm	350–1000 nm	350–2500 nm
10 vs. 30	Control	39	52	70	78	65	35	56	40	96	36	32	48
	RKN	100	100	100	100	100	80	100	100	100	100	100	100
	OA	70	77	85	90	83	58	78	70	98	68	66	74
	Kappa	0.44	0.53	0.70	0.90	0.66	0.15	0.56	0.40	0.96	0.36	0.32	0.48
10 vs. 60	Control	44	55	60	30	25	30	48	36	88	80	24	40
	RKN	100	100	100	100	100	100	100	100	100	100	100	80
	OA	76	80	82	69	67	69	74	68	94	90	62	60
	Kappa	0.48	0.58	0.63	0.32	0.27	0.32	0.48	0.36	0.88	0.8	0.24	0.20

PCA = Principal component analysis; SLDA = Stepwise linear discriminant analysis; FLDA = Fisher's linear discriminant analysis; OA = Overall accuracy.

The performance of the ML classifier with three-dimensionality reduction approaches were tested under two degrees of temporal misalignment between training and testing condition. This helps in understanding the effectiveness of ML classifiers when trained and tested with data collected at various plant growth stages during the cropping season [32]. All spectral signatures measured at 10 days after stress were used to train the ML classifier, which is tested on all spectral signatures obtained at 30 and 60 days after stress in year 1. In year 2, the spectral signatures recorded on 16 days after stress served as training data, which was then tested on the remaining spectral signatures collected on various days after stress. When all the bands were used for training, SLDA showed the best classification accuracies for both 'Rk-Rn-1' and 'M8'. With SLDA, an OA of more than 82% was recorded, with Kappa ranging from 0.63–0.96. With PCA and FLDA, the accuracies were very low. When only a part of the spectral bands (350–1000 nm) was employed to learn ML, overall accuracies and Kappa statistics were decreased. Among the dimensionality reducers, SLDA produced the best accuracies for 350–2500 nm spectral bands and inconclusive results when bands in the 350–1000 nm range were used. A significant confusion between RKN and DS was observed with year 2 data resulting in smaller OA and Kappa with other dimensionality reducers.

Based on the experiments, we observed that RKN stress can be detected at an early stage (10 days after inoculation) from spectral bands in 350–1000 nm and 350–2500 nm by using a basic statistical classifier like ML with a dimensionality reducer. Further experiments need to be conducted to evaluate the ability to detect RKN stress earlier than 10 days after stress. Among the dimensionality reducers, PCA and SLDA work better. Experimental analysis showed that spectral bands in the visual near infrared (VNIR) region (350–1000 nm) are good enough to achieve excellent (>93% OA and Kappa > 0.95) classification accuracy. Temporal alignment experiments showed that RKN stress alone could be detected from ML classifier trained using the data collected at an earlier date. However, when trained with RKN and DS, results are subpar (OA = 60% or less). Based on year 2 results, we observe that both RKN and DS may be successfully differentiated from the control group with excellent OA with VNIR and 350–2500 nm bands. Additional studies are necessary to evaluate the classification accuracy in a larger number of the crop species and to test their robustness under different environmental conditions. In a future study, we intend to repeat these experiments again in a field using a drone-mounted hyperspectral sensor to determine the specific region of the spectral profile that is most informative for predicting various biotic and abiotic stresses.

4. Conclusions

In this study, the genotypes 'Rk-Rn-1'and 'M8' showed differential responses to DS, RKN, and DS + RKN. The magnitude of reduction in response to all three stressors was relatively higher in 'M8' than 'Rk-Rn-1'. The impact of stressors on plant growth followed DS + RKN > DS > RKN. Based on the results, stomatal conductance can be used to distinguish DS and combined DS + RKN stressed plants from non-stressed plants. Though 'Rk-Rn-1' performed better than 'M8' under RKN stress, its genetic potential under drought could be improved to perform better under DS + RKN stress. Leaf reflectance properties exhibited a significant difference between individual stress treatments, indicating that the hyperspectral sensor data can be used to discriminate the nematode infected plants from the drought-stressed plants. The hyperspectral reflectance properties could be used for phenotyping cotton genotypes for RKN, DS or combined stress tolerance after validating under field conditions. Our study reveals that hyperspectral and physiological changes in response to RKN and DS could help diagnose plant health before the plant's visual symptoms appears. In addition, developing cotton varieties with improved tolerance to combined biotic and abiotic stresses is essential to sustain production under varied nematode-infected fields coupled with low rainfall. Furthermore, the methodology used in this study could be adapted to explore different biotic and abiotic stress interactions in cotton and other crops.

Supplementary Materials: The following supporting information can be downloaded at: https://www.mdpi.com/article/10.3390/rs14164021/s1, Figure S1: Drought and nematode infection effect on chlorophyll content (A) and nitrogen balance index (B) of cotton genotypes (Rk-Rn-1 and M8) measured at 16, 24, 32, 46, 53 and 72 days after stress treatment under control, drought stress (DS), nematode stress (RKN), and DS + RKN combination in 2021; Figure S2: Drought and nematode infection effect on transpiration (A) and stomatal conductance (B) of cotton genotypes (Rk-Rn-1 and M8) measured at 16, 24, 32, 46, 53, and 72 days after stress treatment under control, drought stress (DS), nematode stress (RKN), and DS + RKN combination in 2021; Figure S3: Drought and nematode infection effect on total root length (A) and root dry weight (B) of cotton genotypes (Rk-Rn-1 and M8) measured under control (CNT) and nematode stress (RKN) in 2020. Means followed by a common letter are not significantly different by Duncan's multiple range test at the 5% level of significance. Vertical bars denote mean $\pm$ SE.

Author Contributions: Conceptualization, S.S., M.J.W., J.P.B. and R.B.; methodology, S.S., M.J.W. and R.B.; formal analysis, P.R., S.S. and R.M.P.; investigation, S.S., M.J.W. and R.B.; resources, S.S., M.J.W. and R.B.; data curation, P.R., S.S., M.J.W., A.S. and R.B.; writing—original draft preparation, P.R.; writing—review and editing, S.S., M.J.W., J.P.B., R.M.P., K.R.R. and R.B.; visualization, P.R.; supervision, project administration, funding acquisition, S.S., M.J.W., J.P.B. and R.B. All authors have read and agreed to the published version of the manuscript.

Funding: This research was funded by the USDA Agriculture Research Service, Award# 58-6064-9-007 funding to carry out this research and MIS 043050.

Data Availability Statement: Not applicable.

Acknowledgments: We thank undergraduate students at the Plant Stress Physiology Laboratory and USDA-ARS researchers for their help during data collection. The mention of trade names or commercial products in this article is solely for the purpose of providing specific information and does not imply recommendation or endorsement by Mississippi State University or the U.S. Department of Agriculture. The USDA is an equal opportunity provider and employer.

Conflicts of Interest: The authors declare no conflict of interest.

References

1. Robinson, A.F. Reniform in U.S. Cotton: When, Where, Why, and Some Remedies. *Annu. Rev. Phytopathol.* **2007**, *45*, 263–288. [CrossRef] [PubMed]
2. Lawrence, K.S.; Huang, P.; Lawrence, G.W.; Faske, T.; Overstreet, C.; Wheeler, T.; Young, H.; Kemerait, B.; Mehl, H. Nematode Research Report Cotton Varietal and Nematicide Responses in Nematode Soils. In Proceedings of the Beltwide nematode research and education committee 2014, San Antonio, TX, USA, 5–7 January 2015; p. 4.
3. USDA. *Cotton Price Statistics 2020–2021*; Annual Report; United States Department of Agriculture: Memphis, TN, USA, 2021; Volume 102, pp. 1–21. Available online: https://www.ams.usda.gov/mnreports/cnaacps.pdf (accessed on 2 March 2022).
4. Yeates, G.W.; Bongers, T.; De Goede, R.G.M.; Freckman, D.W.; Georgieva, S.S. Feeding Habits in Soil Nematode Families and Genera—An Outline for Soil Ecologists. *J. Nematol.* **1993**, *25*, 315–331. [PubMed]
5. Abad, P.; Gouzy, J.; Aury, J.-M.; Castagnone-Sereno, P.; Danchin, E.G.J.; Deleury, E.; Perfus-Barbeoch, L.; Anthouard, V.; Artiguenave, F.; Blok, V.C.; et al. Genome Sequence of the Metazoan Plant-Parasitic Nematode *Meloidogyne incognita*. *Nat. Biotechnol.* **2008**, *26*, 909–915. [CrossRef]
6. Wasson, A.P.; Ramsay, K.; Jones, M.G.K.; Mathesius, U. Differing Requirements for Flavonoids during the Formation of Lateral Roots, Nodules and Root Knot Nematode Galls in *Medicago truncatula*. *New Phytol.* **2009**, *183*, 167–179. [CrossRef] [PubMed]
7. Kirkpatrick, T.L.; Oosterhuis, D.M.; Wullschleger, S.D. Interaction of Meloidogyne Incognita and Water Stress in Two Cotton Cultivars. *J. Nematol.* **1991**, *23*, 462–467. [PubMed]
8. Ynturi, P.; Jenkins, J.N.; McCarty, J.C., Jr.; Gutierrez, O.A.; Saha, S. Association of Root-Knot Nematode Resistance Genes with Simple Sequence Repeat Markers on Two Chromosomes in Cotton. *Crop Sci.* **2006**, *46*, 2670–2674. [CrossRef]
9. Ralmi, N.H.A.A.; Khandaker, M.M.; Mat, N. Occurrence and Control of Root Knot Nematode in Crops: A Review. *Aust. J. Crop Sci.* **2016**, *10*, 1649–1654. [CrossRef]
10. Pulavarty, A.; Egan, A.; Karpinska, A.; Horgan, K.; Kakouli-Duarte, T. Plant Parasitic Nematodes: A Review on Their Behaviour, Host Interaction, Management Approaches and Their Occurrence in Two Sites in the Republic of Ireland. *Plants* **2021**, *10*, 2352. [CrossRef]
11. Barbary, A.; Djian-Caporalino, C.; Marteu, N.; Fazari, A.; Caromel, B.; Castagnone-Sereno, P.; Palloix, A. Plant Genetic Background Increasing the Efficiency and Durability of Major Resistance Genes to Root-Knot Nematodes Can Be Resolved into a Few Resistance QTLs. *Front. Plant Sci.* **2016**, *7*, 632. [CrossRef]
12. Roberts, P.A. Current Status of the Availability, Development, and Use of Host Plant Resistance to Nematodes. *J. Nematol.* **1992**, *24*, 213–227.
13. Sikder, M.M.; Vestergård, M. Impacts of Root Metabolites on Soil Nematodes. *Front. Plant Sci.* **2020**, *10*, 1792. [CrossRef] [PubMed]
14. Suzuki, N.; Rivero, R.M.; Shulaev, V.; Blumwald, E.; Mittler, R. Abiotic and Biotic Stress Combinations. *New Phytol.* **2014**, *203*, 32–43. [CrossRef] [PubMed]
15. Cotton Incorporated Irrigation Management—Why Irrigate Cotton? Available online: https://www.cottoninc.com/cotton-production/ag-resources/irrigation-management/why-irrigate-cotton/ (accessed on 2 March 2022).
16. McDonald, R.I.; Girvetz, E.H. Two Challenges for U.S. Irrigation Due to Climate Change: Increasing Irrigated Area in Wet States and Increasing Irrigation Rates in Dry States. *PLoS ONE* **2013**, *8*, e65589. [CrossRef]
17. Qi, J.; Wang, J.; Gong, Z.; Zhou, J.-M. Apoplastic ROS Signaling in Plant Immunity. *Curr. Opin. Plant Biol.* **2017**, *38*, 92–100. [CrossRef]
18. Mittler, R.; Blumwald, E. Genetic Engineering for Modern Agriculture: Challenges and Perspectives. *Annu. Rev. Plant Biol.* **2010**, *61*, 443–462. [CrossRef] [PubMed]
19. Atkinson, N.J.; Urwin, P.E. The Interaction of Plant Biotic and Abiotic Stresses: From Genes to the Field. *J. Exp. Bot.* **2012**, *63*, 3523–3543. [CrossRef] [PubMed]
20. Eisenback, J.D.; Dodge, D.J. Description of a Unique, Complex Feeding Socket Caused by the Putative Primitive Root-Knot Nematode, *Meloidogyne kikuyensis*. *J. Nematol.* **2012**, *44*, 148–152.
21. Holbein, J.; Franke, R.B.; Marhavý, P.; Fujita, S.; Górecka, M.; Sobczak, M.; Geldner, N.; Schreiber, L.; Grundler, F.M.W.; Siddique, S. Root Endodermal Barrier System Contributes to Defence against Plant-Parasitic Cyst and Root-Knot Nematodes. *Plant J.* **2019**, *100*, 221–236. [CrossRef]
22. Davis, R.F.; Earl, H.J.; Timper, P. Effect of Simultaneous Water Deficit Stress and *Meloidogyne incognita* Infection on Cotton Yield and Fiber Quality. *J. Nematol.* **2014**, *46*, 108–118.
23. Kirkpatrick, T.L.; Van Iersel, M.W.; Oosterhuis, D.M. Influence of *Meloidogyne incognita* on the Water Relations of Cotton Grown in Microplots. *J. Nematol.* **1995**, *27*, 465–471.
24. Reddy, K.R.; Hodges, H.F.; McKinion, J.M. Crop Modeling and Application: A Cotton Example. In *Advances in Agronomy*; Academic Press: Cambridge, MA, USA, 1997; ISBN 978-0-08-056372-5.
25. Lu, P.; Davis, R.F.; Kemerait, R.C.; van Iersel, M.W.; Scherm, H. Physiological Effects of Meloidogyne Incognita Infection on Cotton Genotypes with Differing Levels of Resistance in the Greenhouse. *J. Nematol.* **2014**, *46*, 352–359. [PubMed]
26. Carneiro, R.G.; Mazzafera, P.; Ferraz, L.C.C.B.; Muraoka, T.; Trivelin, P.C.O. Uptake and Translocation of Nitrogen, Phosphorus and Calcium in Soybean Infected with *Meloidogyne incognita* and *M. Javanica*. *Fitopatol. Bras.* **2002**, *27*, 141–150. [CrossRef]
27. Walker, N.R.; Kirkpatrick, T.L.; Rothrock, C.S. Interaction between *Meloidogyne incognita* and *Thielaviopsis basicola* on Cotton (*Gossypium hirsutum*). *J. Nematol.* **1998**, *30*, 415–422.

28. Bock, C.H.; Poole, G.H.; Parker, P.E.; Gottwald, T.R. Plant Disease Severity Estimated Visually, by Digital Photography and Image Analysis, and by Hyperspectral Imaging. *Crit. Rev. Plant Sci.* **2010**, *29*, 59–107. [CrossRef]
29. Lowe, A.; Harrison, N.; French, A.P. Hyperspectral Image Analysis Techniques for the Detection and Classification of the Early Onset of Plant Disease and Stress. *Plant Methods* **2017**, *13*, 80. [CrossRef]
30. Wong, C.Y.S.; Gamon, J.A. Three Causes of Variation in the Photochemical Reflectance Index (PRI) in Evergreen Conifers. *New Phytol.* **2015**, *206*, 187–195. [CrossRef]
31. Sun, S.; Zhou, Y.; Chen, J.; Shi, J.; Zhao, H.; Zhao, H.; Song, W.; Zhang, M.; Cui, Y.; Dong, X.; et al. Extensive Intraspecific Gene Order and Gene Structural Variations between Mo17 and Other Maize Genomes. *Nat. Genet.* **2018**, *50*, 1289–1295. [CrossRef]
32. Samiappan, S.; Bheemanahalli, R.; Zhou, M.; Brooks, J.; Wubben, M. Early Detection of Root-Knot Nematode (*Meloidogyne incognita*) Infestation in Cotton Using Hyperspectral Data. In Proceedings of the 2021 IEEE International Geoscience and Remote Sensing Symposium IGARSS, Brussels, Belgium, 11–16 July 2021; pp. 5849–5852.
33. Grzybowski, M.; Wijewardane, N.K.; Atefi, A.; Ge, Y.; Schnable, J.C. Hyperspectral Reflectance-Based Phenotyping for Quantitative Genetics in Crops: Progress and Challenges. *Plant Commun.* **2021**, *2*, 100209. [CrossRef]
34. Behmann, J.; Steinrücken, J.; Plümer, L. Detection of Early Plant Stress Responses in Hyperspectral Images. *ISPRS J. Photogramm. Remote Sens.* **2014**, *93*, 98–111. [CrossRef]
35. Gitelson, A.A.; Kaufman, Y.J.; Merzlyak, M.N. Use of a Green Channel in Remote Sensing of Global Vegetation from EOS-MODIS. *Remote Sens. Environ.* **1996**, *58*, 289–298. [CrossRef]
36. Delalieux, S.; Somers, B.; Verstraeten, W.W.; van Aardt, J.A.N.; Keulemans, W.; Coppin, P. Hyperspectral Indices to Diagnose Leaf Biotic Stress of Apple Plants, Considering Leaf Phenology. *Int. J. Remote Sens.* **2009**, *30*, 1887–1912. [CrossRef]
37. Melandri, G.; Thorp, K.R.; Broeckling, C.; Thompson, A.L.; Hinze, L.; Pauli, D. Assessing Drought and Heat Stress-Induced Changes in the Cotton Leaf Metabolome and Their Relationship with Hyperspectral Reflectance. *Front. Plant Sci.* **2021**, *12*, 751868. [CrossRef] [PubMed]
38. Calzone, A.; Cotrozzi, L.; Lorenzini, G.; Nali, C.; Pellegrini, E. Hyperspectral Detection and Monitoring of Salt Stress in Pomegranate Cultivars. *Agronomy* **2021**, *11*, 1038. [CrossRef]
39. Chen, J.J.; Zhen, S.; Sun, Y. Estimating Leaf Chlorophyll Content of Buffaloberry Using Normalized Difference Vegetation Index Sensors. *HortTechnology* **2021**, *31*, 297–303. [CrossRef]
40. Prasad, S.; Kalluri, H.; Bruce, L.M.; Samiappan, S. Data Dependent Adaptation for Improved Classification of Hyperspectral Imagery. In Proceedings of the 2010 IEEE International Geoscience and Remote Sensing Symposium, Honolulu, HI, USA, 25–30 July 2010; pp. 68–71.
41. Samiappan, S.; Prasad, S.; Bruce, L.M.; Robles, W. NASA's Upcoming HyspIRI Mission—Precision Vegetation Mapping with Limited Ground Truth. In Proceedings of the 2010 IEEE International Geoscience and Remote Sensing Symposium, Honolulu, HI, USA, 25–30 July 2010; pp. 3744–3747.
42. Melgani, F.; Bruzzone, L. Classification of Hyperspectral Remote Sensing Images with Support Vector Machines. *IEEE Trans. Geosci. Remote Sens.* **2004**, *42*, 1778–1790. [CrossRef]
43. Cheriyadat, A.; Bruce, L.M. Why Principal Component Analysis Is Not an Appropriate Feature Extraction Method for Hyperspectral Data. In Proceedings of the IGARSS 2003, 2003 IEEE International Geoscience and Remote Sensing Symposium (IEEE Cat. No.03CH37477), Toulouse, France, 21–25 July 2003; Volume 6, pp. 3420–3422.
44. Du, Q.; Younan, N.H. Dimensionality Reduction and Linear Discriminant Analysis for Hyperspectral Image Classification. In Proceedings of the Knowledge-Based Intelligent Information and Engineering Systems, Zagreb, Croatia, 3–5 September 2008; Lovrek, I., Howlett, R.J., Jain, L.C., Eds.; Springer: Berlin/Heidelberg, Germany, 2008; pp. 392–399.
45. Duda, R.O.; Hart, P.E.; Stork, G.E. *Pattern Classification*, 2nd ed.; Wiley Inter-Science: New York, NY, USA, 2000.
46. Prasad, S.; Bruce, L.M. Overcoming the Small Sample Size Problem in Hyperspectral Classification and Detection Tasks. In Proceedings of the IGARSS 2008—2008 IEEE International Geoscience and Remote Sensing Symposium, Boston, MA, USA, 6–11 July 2008; Volume 5, pp. V-381–V-384.
47. McCarty, J.C., Jr.; Jenkins, J.N.; Wubben, M.J.; Hayes, R.W.; Callahan, F.E.; Deng, D. Registration of Six Germplasm Lines of Cotton with Resistance to the Root-Knot and Reniform Nematodes. *J. Plant Regist.* **2017**, *11*, 168–171. [CrossRef]
48. Hussey, R.; Barker, K. A Comparison of Methods of Collecting Inocula of *Meloidogyne* spp., Including a New Technique. *Plant Dis. Rep.* **1973**, *57*, 1025–1028.
49. Foody, G.M. Status of Land Cover Classification Accuracy Assessment. *Remote Sens. Environ.* **2002**, *80*, 185–201. [CrossRef]
50. da Silva, E.C.; Nogueira, R.J.; Silva, M.; Albuquerque, M. Drought Stress and Plant Nutrition. *Plant Stress* **2010**, *5*, 32–41.
51. Giunta, F.; Motzo, R.; Deidda, M. SPAD Readings and Associated Leaf Traits in Durum Wheat, Barley and Triticale Cultivars. *Euphytica* **2002**, *125*, 197–205. [CrossRef]
52. Nafady, N.A.; Sultan, R.; El-Zawahry, A.M.; Mostafa, Y.S.; Alamri, S.; Mostafa, R.G.; Hashem, M.; Hassan, E.A. Effective and Promising Strategy in Management of Tomato Root-Knot Nematodes by *Trichoderma harzianum* and Arbuscular Mycorrhizae. *Agronomy* **2022**, *12*, 315. [CrossRef]
53. Ding, L.; Lu, Z.; Gao, L.; Guo, S.; Shen, Q. Is Nitrogen a Key Determinant of Water Transport and Photosynthesis in Higher Plants upon Drought Stress? *Front. Plant Sci.* **2018**, *9*, 1143. [CrossRef] [PubMed]

54. Chen, D.; Wang, S.; Cao, B.; Cao, D.; Leng, G.; Li, H.; Yin, L.; Shan, L.; Deng, X. Genotypic Variation in Growth and Physiological Response to Drought Stress and Re-Watering Reveals the Critical Role of Recovery in Drought Adaptation in Maize Seedlings. *Front. Plant Sci.* **2016**, *6*, 1241. [CrossRef] [PubMed]
55. Ramamoorthy, P.; Bheemanahalli, R.; Meyers, S.L.; Shankle, M.W.; Reddy, K.R. Drought, Low Nitrogen Stress, and Ultraviolet-B Radiation Effects on Growth, Development, and Physiology of Sweetpotato Cultivars during Early Season. *Genes* **2022**, *13*, 156. [CrossRef]
56. Zhao, D.; Reddy, K.R.; Kakani, V.G.; Reddy, V.R. Nitrogen Deficiency Effects on Plant Growth, Leaf Photosynthesis, and Hyperspectral Reflectance Properties of Sorghum. *Eur. J. Agron.* **2005**, *22*, 391–403. [CrossRef]
57. Collalti, A.; Tjoelker, M.G.; Hoch, G.; Mäkelä, A.; Guidolotti, G.; Heskel, M.; Petit, G.; Ryan, M.G.; Battipaglia, G.; Matteucci, G.; et al. Plant Respiration: Controlled by Photosynthesis or Biomass? *Glob. Change Biol.* **2020**, *26*, 1739–1753. [CrossRef]
58. Zhang, H.; Sonnewald, U. Differences and Commonalities of Plant Responses to Single and Combined Stresses. *Plant J.* **2017**, *90*, 839–855. [CrossRef]
59. Zhang, P.; Bonte, D.; De Deyn, G.B.; Vandegehuchte, M.L. Belowground Plant-Plant Signaling of Root Infection by Nematodes. *Pedobiologia* **2020**, *83*, 150688. [CrossRef]
60. Zhang, P.; Bonte, D.; De Deyn, G.B.; Vandegehuchte, M.L. Leachates from Plants Recently Infected by Root-Feeding Nematodes Cause Increased Biomass Allocation to Roots in Neighbouring Plants. *Sci. Rep.* **2021**, *11*, 2347. [CrossRef]
61. Zhang, L.; Zhang, J.; Christie, P.; Li, X. Pre-Inoculation with Arbuscular Mycorrhizal Fungi Suppresses Root Knot Nematode (*Meloidogyne incognita*) on Cucumber (*Cucumis sativus*). *Biol. Fertil. Soils* **2008**, *45*, 205. [CrossRef]
62. Cohen, J. A Coefficient of Agreement for Nominal Scales. *Educ. Psychol. Meas.* **1960**, *20*, 37–46. [CrossRef]